Anisotropic Behaviour of an Overconsolidated Clay

Le Comportement Anisotrope d'Argile Surconsolidée

K.STARZEWSKI Senior Lecturer, Dept. of Civil Eng. of the Univ. of Aston in Birmingham,
C.P.THOMAS Geotechnical Engineer, Geotechnical Engineering Ltd., Gloucester, U.K.

SYNOPSIS

Stress-deformation behaviour of block and core samples of a heavily overconsolidated Lias clay (estimated in situ K_o of approximately 3.0) are presented for several different loading paths. It is shown that the volumetric-axial strain relationships are approximately linear and that the soil exhibits a high degree of anisotropy. It is further shown that the "elastic" parameters governing the strain ratios are sensibly constant for the different loading paths: results obtained from consolidated drained tests on vertical and horizontal samples were used to predict the behaviour of the soil in incremental hydrostatic compression tests, incremental anisotropic (orthotropic) compression tests and orthotropic compression tests at a constant stress ratio. The same "elastic" parameters were used for prediction of the undrained "elastic" modulus of the soil and pore pressure parameter A.

INTRODUCTION

Some interesting results are presented from a laboratory study of the mechanical properties of the heavily overconsolidated Lower Lias Clay (Thomas 1973). The basic aim of the study was to determine: (i) the in situ K_o value, (ii) the basic parameters governing the axial and volumetric compressibility of the Lias under a variety of stress paths, (iii) the consolidation characteristics and (iv) the effect of sampling method (disturbance) on the measured parameters, from both triaxial and oedometer laboratory testing. The presented results fall within (ii), above, and are based on several series of triaxial tests loaded under the stress paths, shown in Fig.1, and are as follows: (a) TDV, TDH and TD2 - consolidated drained compression tests, Fig.1(a); (b) TC - incremental hydrostatic (isotropic) compression tests, Fig.1(c); (c) TA1 and TA2, - incremental anisotropic (orthotropic) compression tests, Fig.1(b) and (d) TA3 - orthotropic drained compression tests at a constant incremental stress ratio, Fig.1(c).

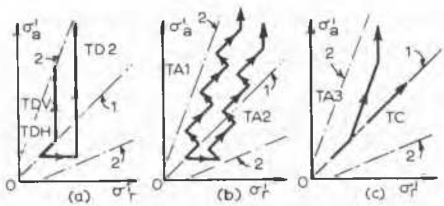

Fig.1 Effective Stress Paths: σ'_a vs σ'_r
1 - Isotropic path, 2 - Failure Envelopes

The tests were carried out on 70mm undisturbed hand trimmed block, cored and tube samples. The results of the tube samples are shown in the figures but are not discussed in the text. The block, cored and tube samples are identified on the figures by B, C and T respectively following the test number.

The samples used in the tests were obtained from the clay pit of the Northcot Brickworks, Blockley, Gloucestershire. The sampled horizon lies near the top of the Lower Lias deposits. The estimated overburden at this locality was in the order of 500-700m.

The tube and cored samples were obtained from three boreholes (sunk using waterflush rotary core drilling) positioned at 1m spacing in a triangular pattern. The block samples were obtained from an excavation made in the face of the quarry, as close as possible to the boreholes. A specially designed probe was used to measure the in situ pore pressures for estimation of the effective overburden stresses.

Physical Properties: The following physical properties were recorded: water content - 16% to 22%, mean 18.4%; liquid limit 53 to 63%, mean 59%; plastic limit 25 to 29%, mean 27%; shrinkage limited 15 to 15.5%, minerology of the clay (Coulthard 1975) 80-90% clay, consisting mainly of Illite and Kaolin, with 5% Quartz, 2.6% Pyrite, up to 2% Calcite and up to 2% organic matter; specific gravity of solids 2.67 to 2.75, mean 2.72.

Equilibrium stress σ'_k and K_o: The equilibrium stress, measured in the triaxial and oedometer apparatus varied widely, but a mean value for σ'_k/σ'_{ov} of 1.8 was obtained. The results of the triaxial testing indicated that the pore pressure parameter A was in the range of 0.55 to 0.65. For an A value in this range and a σ'_k/σ'_{ov} of 1.8 ± 10%, the K_o value lies between 2.4 and 3.8, with a mean value of 3.0.

TEST RESULTS

Details of the laboratory testing apparatus and testing procedures are beyond the scope of this paper and are described elsewhere (Thomas 1973). In brief, tests in the TD2 and TA2 series were carried out in a specially developed Independent Stress Cell, whereas the other tests were carried out in an ordinary 100mm triaxial cell modified for 70mm diameter samples.

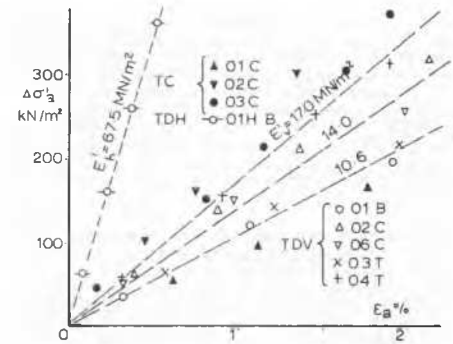

Fig.2 Incremental Axial Stress vs Axial Strain for TDV, TDH & TC Tests

In all tests axial and volumetric deformations were recorded together with the applied stresses and pore pressures. Drainage was radial only, into filter paper strips, and pores pressures were measured at the centre of the top of the sample during drained and undrained loading.

CONSOLIDATED DRAINED TRIAXIAL TESTS

These tests are subdivided into three series TDV, TDH and TD2 - see Fig.1(a). The former two series were carried out on vertical and horizontal samples respectively. The latter series, TD2 was performed on vertical samples in the new cell.

TDV Series. This series consisted of three tests on vertical block and core samples. In each case the specimen was loaded at a constant rate of strain, following initial isotropic consolidation. The results are summarized in Figs 2 and 3. It is seen that the stress-strain curves and the strain paths are virtually linear up to approximately 1% axial strain.

TDH Series. This series was unfortunately reduced to a single test on a small (38mm diameter) block sample because of the difficulties in preparation of the test specimens; The results of the test are plotted in Figs. 2 and 3. The stress-strain graph beyond the 'bedding' correction (not shown) is approximately linear with the slope which is seen to be considerably greater than for TDV series. The corrected strain path is also linear up to 0.8% axial strain.

TD2 Series. This series consisted of two tests, one on each type of sample. Each sample was initially consolidated to an effective stress ratio K of approximately 1.7. The specimen was then loaded as per the TDV series, at the same rates of strain.

The results from this series of tests (not presented in this paper) are rather limited, however they indicate that the axial deformation modulus is high when reloading to K=1 condition, beyond which the results are comparable with the TDV series.

Elastic Analysis (TDV TDH & TD2 Series). It has been seen from these results that the stress-strain relationships are approximately linear; this is also true of the strain paths up to a stress ratio (1/K) of approximately 2. The unloading stages (not illustrated) show that the strains are not fully recoverable and therefore the material is not elastic. However, if it is considered that the material behaves linearly, it may be treated as a linearly pseudo-elastic material during loading. The results from the horizontal test show that the material has a greater stiffness in the horizontal direction than in the vertical i.e. it is anisotropic. It is reasonable to assume, however, that for this type of deposit the horizontal plane would be an isotropic plane (Barden 1963) and thus the results are studied in the terms of "orthotropic" elasticity.

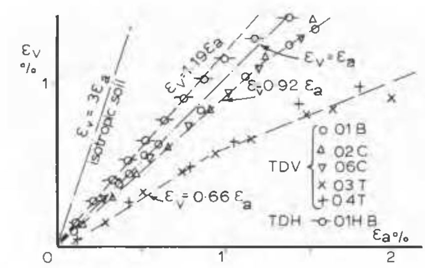

Fig.3 Strain Paths for TDV and TDH Tests

ORTHOTROPIC ELASTIC CONSTANTS

The general stress-strain relationships for an orthotropic elastic material under principal stress increments are given in the Appendix. It is seen that the deformation of vertical and horizontal samples is dependent on four elastic constants, $E'_v, n, \nu_{hv}, \nu_{hh}$. In order to determine these constants it is necessary to analyse the results of tests on the vertical and horizontal samples together.

In the case of consolidated drained tests, the vertical Young's modulus E'_v is numerically equal to the axial deformation modulus $(\Delta\sigma'_a/\varepsilon_a)$ for a vertical sample whereas the horizontal Young's modulus E'_h is numerically equal to the axial deformation modulus of a horizontal sample. From results in Fig.2 E'_v varies between 10.6-17.0 MN/m^2 and E'_h is of the order of 67.5 MN/m^2: hence the modulus ratio n lies between 6.37 and 3.97. However, as E'_h was determined from a test on a small diameter sample, it is considered that this would be the upper limit for E'_h and therefore that the higher value of E'_v should be used to compute the modulus ratio 'n', i.e. n = 3.97. The two Poisson's ratios ν_{hv} and ν_{hh} are determined from equations (A1) and (A2) using the strain ratios of the two vertical and horizontal samples respectively.

With a strain ratio of 0.92 (for vertical samples, Fig.3) a surprisingly low value of ν_{hv} = 0.04 is obtained. The Poisson's ratio ν_{hh} is obtained using a strain ratio of 1.19 (horizontal sample - Fig.3), n of 3.97 and ν_{hv} of 0.04: a further surprising result that ν_{hh} = -0.349 is obtained. The results satisfy the criterion for positive strain energy (Pickering 1970).

UNDRAINED PARAMETERS

Undrained triaxial compression tests have not been carried out although undrained stages are included in the TA1 and TA2 series. However as the material behaves "elastically" the undrained behaviour can be predicted. If an increase of total axial stress $\Delta\sigma_a$ is applied in an undrained manner, then the axial deformation is given by $\varepsilon_a = \Delta\sigma_a/E_{uv}$ where E_{uv} is the undrained vertical Young's modulus.

For a saturated clay the axial deformation may also be expressed in terms of the effective stresses and orthotropic "elastic" parameters; with the aid of the pore pressure coefficient A:

$$\varepsilon_a = (\Delta\sigma'_a - 2\nu_{hv}\Delta\sigma'_r)/E'_v \quad \ldots\ldots\ldots(1)$$

where $\Delta\sigma'_a = (1-A)\Delta\sigma_a$
and $\Delta\sigma'_r = (-A)\Delta\sigma_a$, hence

$$\varepsilon_a = [(1-A) + 2\nu_{hv}A]\Delta\sigma_a/E'_v \quad \ldots\ldots\ldots(2)$$

and $E_{uv} = \Delta\sigma_a/\varepsilon_a = E'_v/[1 - A(1-2\nu_{hv})] \ldots\ldots(3)$

But the pore pressure coefficient A can also be expressed in terms of the orthotropic elastic parameters (Pickering 1970):

$$A = (1-2\nu_{hv})/[1 - 4\nu_{hv} + 2(1-\nu_{hh})/n] \ldots\ldots(4)$$

Therefore, using the range of parameters determined earlier, the undrained modulus for core or block samples is given by

$$E_{uv} = 2.26E'_v \text{ to } 3.03E'_v \ldots\ldots\ldots(5)$$

INCREMENTAL SPHERICAL LOADING (TC SERIES)

The TC series was carried out on three short (H/D = 1) cored samples. Throughout the tests the axial and volumetric strains were recorded together with the cell and pore water pressures. The results are summarised in Figs 2 and 4. Each increment of cell pressure was applied under undrained conditions and the pore pressure allowed to equalise before the drainage tap was opened; the pore pressure parameter B measured in tests O2C and O3C was greater than 0.90 whereas in test O1C it was only in the order of 0.5.

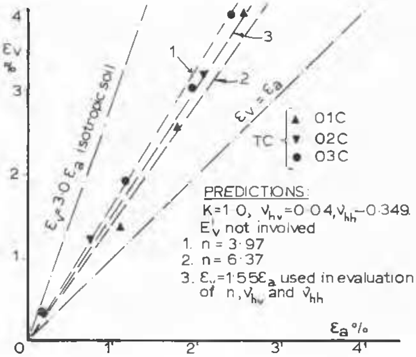

Fig.4 Strain Paths for TC Tests

The stress-strain relationship seen in Fig.2 is approximately linear up to 2% axial strain, beyond this level it becomes progressively steeper (not shown in Fig.2). The strain results correlate closely (Fig.4) and prove to be remarkably linear over the full range giving a strain ratio of 1.55. This result suggests that the material is behaving "elastically" but exhibits marked anisotropy since the strain ratio deviates significantly from the isotropic value of 3.

Elastic Predictions and Analysis. The deformation of the sample under the applied stresses is considered below in terms of the orthotropic elastic constants derived from the TD series. These values will then be considered in the light of the results obtained from this series of tests.

The axial deformation is given by equation (A1) in which, for the case of hydrostatic loading, $\bar{K}$ = 1. With the small value of ν_{hv} (0.04) the predicted plots of the incremental axial stress against axial strain are almost identical to the ones obtained for the TDV tests (Fig.2); it can be seen that for tests O2 and O3 the elastic predictions are slightly on the low side.

The strain ratio, for the hydrostatic loading case is obtained from equation (A4) by putting $\bar{K}$ = 1.0; the range of the predictions is shown in Fig.4. The agreement is good and demonstrates that the values obtained from the TD series, where $\bar{K}$ = 0, are equally applicable to this series where $\bar{K}$ = 1. This confirms that within the stress range considered the material behaves as linearly "elastic" material and may be expected to do so for any stress paths between $\bar{K}$ = 0 and $\bar{K}$ = 1.

It was seen from the TD series that the Young's modulus E'_v varied considerably, and thus a range of values of the modulus ratio, n, was obtained. It is now possible to evaluate ν_{hv}, ν_{hh} and n from the three sets of strain ratios which are far more consistant than the deformation modulus. Substituting into equation (A4) the experimental strain ratios for the TDV, TDH and TC tests, respectively, we obtain three simultaneous equations in terms of ν_{hv}, ν_{hh} and n. On solution of these three equations we obtain $\nu_{hv} = 0.04$, $\nu_{hh} = -0.38$ and $n = 4.70$. Thus n is found to be higher than the initially assumed value of 3.97 but is within the range suggested by the recorded vertical and horizontal Young's moduli in the TD series. The Poisson's ratio ν_{hv} remains unaltered and ν_{hh} is only slightly adjusted. These values thus satisfy the strain ratios for the stress increment ratios, $\bar{K}$, at 0 and 1, in the range of axial to radial effective stress ratio (1/K) of 1 to 2.

CONSTANT STRESS INCREMENT RATIO TESTS (TA3 SERIES)

A series of three triaxial tests was performed where the axial and radial stresses were both increased continuously at a constant stress increment ratio - see Fig.1(c). The rate of loading was governed to allow the sample to follow a fully drained stress path.

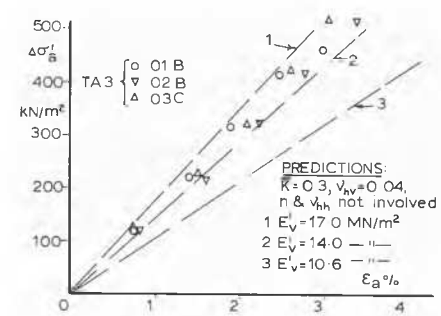

Fig.5 TA3 Test $\Delta\sigma'_a$ vs ε_a Plot

It was found to be difficult to maintain a constant effective stress increment ratio ($\bar{K}$) and in practice the ratio varied between 0.25 and 0.36 over the three tests. The stress-strain results are plotted collectively in Fig.5 and it is seen that the results correlate reasonably well. In the early stage the relationship is approximately linear but the slope is seen to be increasing with increase of stress. The strain paths are shown in Fig.6.

Elastic Predictions and Analysis. The axial stress-strain relationship and the strain ratio is considered using the parameters determined from the TD and TC series and is compared with the observed results in Fig 5 and 6. A general case is considered with the incremental stress ratio $\bar{K} = 0.30$, as this is an average value of $\bar{K}$ for this series of tests. Up to approximately 2% axial strain the observed strains are sensibly predicted using the upper range of the Young's modulus values from the TD series (Fig.5). There is also a reasonable correlation between the experimental and predicted strain paths (Fig.6). It is therefore seen that the numerical values of ν_{hv}, ν_{hh} and n predicted from the TD and TC series are also applicable to the TA3 series.

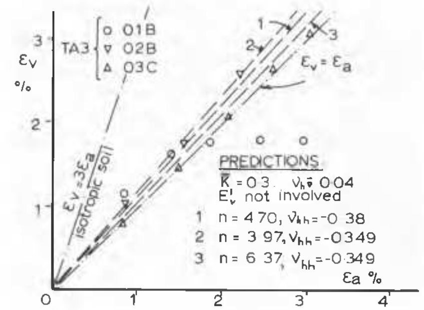

Fig.6. Strain Paths for TA3 Tests

INCREMENTAL LOADING TESTS (TA1 and TA2 SERIES)

Two series of tests were carried out where the samples were incrementally loaded. In the first series (TA1) the specimens were initially consolidated under hydrostatic stress, whereas in the second series (TA2) the samples were initially consolidated to a stress condition where the radial stress was greater than the axial stress - Fig.1(b).

TA1 Series. This series consisted of five tests on block and core samples. Each sample was subjected to a series of increments of axial and radial stresses at a ratio 3:1. The increments were initially applied under undrained conditions; the magnitude of the increments was selected to avoid failure at this stage. The samples were then allowed to consolidate into a back pressure - the end-of-consolidation stresses lie on a stress path approximately equivalent to that of the TA3 series (see Fig.1b).

During the undrained loading an excess pore pressure is induced, which for a saturated clay is dependent only on the pore pressure parameter A (Skempton 1954). The magnitude of A is reflected by the slope of the undrained portion of the effective stress paths. The slopes of the undrained effective stress paths for the block and core samples are generally similar (not shown) and the measured A values are generally of the order of 0.55 to 0.67 (Fig.7).

A fairly wide scatter of results is evident but it is seen that the general trend is for

A to decrease as the effective stress ratio (1/K) increases. Similar results have been reported by Som (1968) for London Clay. The results in Fig.8 also show a considerable amount of scatter. However, it is observed that the individual sets of results fall on smooth lines of approximately similar slope, which increases with increase of stress level. In general, the end-of-consolidation strain paths (Fig.9) fall below $\varepsilon_v = \varepsilon_a$ line; the strain ratios for the block and core samples are 0.99 and 0.86 respectively. The slope of the consolidation strain path (not shown) was observed to be in the region of 1.5 to 1.6.

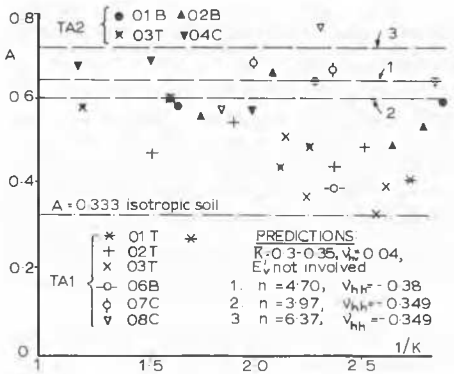

Fig. 7 Plot of A vs $1/K = \sigma_a'/\sigma_r'$

During the consolidation stage the change of stress is hydrostatic as it is solely due to the dissipation of pore pressure. It is therefore interesting to note that despite considerable undrained deformation the core and block samples yield the same results as the TC series where $\varepsilon_v = 1.55\,\varepsilon_a$.

TA2 Series. In this series of three tests the samples were initially reconsolidated to K in the order of 1.5 to 1.7. The samples were then loaded with incremental loadings similar to the TA1 Series (Fig.1(b)) but not so close to the failure envelope in the undrained stages. The immediate deformations were, therefore, smaller than in the TA1 series.

The values of the pore pressure parameter A obtained from the undrained stages of the tests are generally between 0.5 and 0.7 as can be seen in (Fig.7). There is a considerable scatter of results but they generally follow the trend indicated by TA1 series.

The results in Fig.8 show some scatter, and there is a general trend for the axial deformation modulus $(\Delta\sigma_a'/\varepsilon_a)$ to increase with increase of the stress level. The strains at the end of consolidation are plotted in Fig.9: the results indicate that due to the smaller undrained deformation the strain ratio from this series is generally greater than for the TA1 series. The slopes of the strain paths during the consolidation stage, where the stress path is isotropic, are of the same order as for TA1 series (not shown).

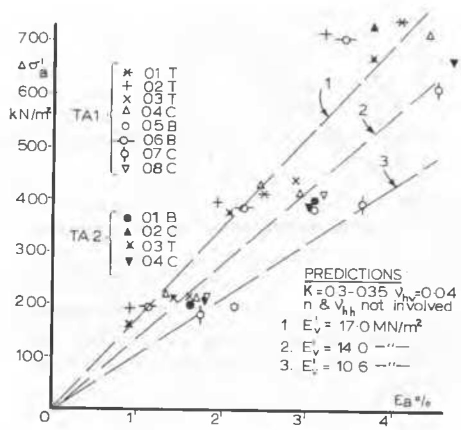

Fig.8 TA1 and TA2 Tests: $\Delta\sigma_a'$ vs ε_a

Elastic Predictions and Analysis. The results of previous tests have shown that the Lias clay is behaving as an orthotropic linearly "elastic" material during initial loading. For such a material it may be expected that the pore pressure parameter A, varies considerably from the isotropic elastic value of one third. Substituting the values of n, ν_{hv} and ν_{hh} obtained from TD and TC series on core and block samples into equation (4) the value of A is found to vary between 0.61 and 0.73; the predictions fit reasonably well amongst the scattered experimental results as shown in Fig.7. The predicted stress-strain relationships for the end of consolidation condition for each stage is shown in Fig.8. For the TA1 series this is seen to give a reasonable upper bound fit for the first two increments, beyond which the predicted strains are greater than the observed. Similar results are also shown for the TA2 series. A better fit may be obtained if E_v' was expressed as some function of the effective radial stress. The slopes of the strain paths during consolidation were seen to be (not shown) equivalent to that of the TC series for the cored and block samples indicating that during consolidation the samples behaved "elastically". The predicted end-of-consolidation strain paths are shown in Fig.9. It is seen that for the TA1 series all the experimental results fall below the predicted; in the TA2 series the experimental paths are not so widely scattered but still fall below the predicted results; in general, the strain ratios are not predicted well by the elastic theory.

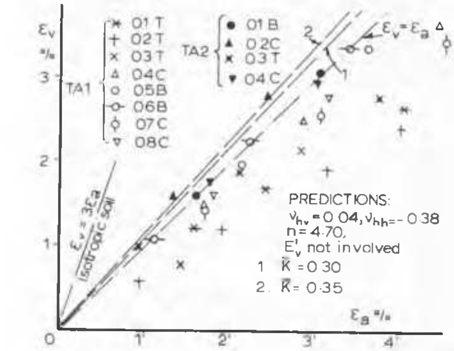

Fig.9 Strain Paths for TA1 and TA2 Tests

This would appear to be due to the undrained loading stage where samples, particularly in the TA1 series, were close to failure, therefore taking the sample beyond its limit of linearity.

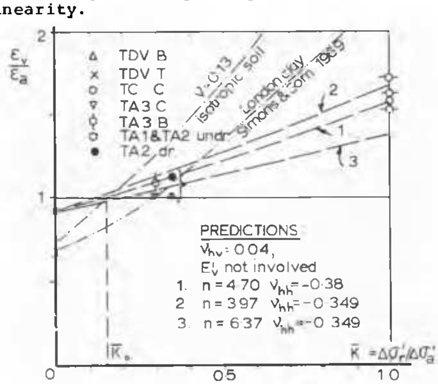

Fig.10 Strain ratio $\varepsilon_v/\varepsilon_a$ vs $\bar{K} = \Delta\sigma'_r/\Delta\sigma'_a$

OVERALL ANALYSIS OF RESULTS

The stress-strain behaviour of block and core samples of Lias clay have been presented for several different loading paths. It has been shown that the volumetric-axial strain relationships are approximately linear. Analysis of the individual series of tests has shown that the soil exhibits a high degree of anisotropy. It has further been shown that the "elastic" parameters governing the strain ratios are sensibly constant from one series of tests to another; a summary of the experimental results and predictions is shown in Fig.10. The vertical, effective stress, Young's Modulus, E'_v varied considerably from sample to sample but a mean value of 14 MN/m^2 can be inferred with the other elastic constants as follows: $n = 4.70$, $\nu_{hv} = 0.04$, $\nu_{hh} = -0.38$, $A = 0.65$ and $E_{uv} = 34$ MN/m^2.

APPENDIX

Stress-strain relationships for an orthotropic elastic material with vertical axes of symmetry.

The relevant elastic constants are:
E'_v - vertical, effective stress, Young's modulus, E'_h - horizontal, effective stress, Young's modulus, ν_{hv}, ν_{vh}, ν_{hh} - Poisson's ratios for effects of strains in the direction of the first suffix on the strains in the direction of the second suffix;
$n = E'_h/E'_v$ = the modulus ratio.

From consideration of energy $\nu_{vh} = n\nu_{hv}$
Axial and radial strains due to application of axial and radial stress increments $\Delta\sigma'_a$ and $\Delta\sigma'_r = \bar{K}\Delta\sigma'_a$ on a vertical sample are given respectively, by

$$\varepsilon_a = \Delta\sigma'_a(1-2\nu_{hv}\bar{K})/E'_v \quad \text{(A1)}$$

and $$\varepsilon_r = \Delta\sigma'_a[\bar{K}(1-\nu_{hh})/n - \nu_{hv}]/E'_v \quad \text{(A2)}$$

and the volumetric strain by

$$\varepsilon_v = \Delta\sigma'_a[1-2\nu_{hv}+2\bar{K}(1-\nu_{hh}-n\nu_{hv})/n]/E'_v \quad \text{(A3)}$$

The strain ratio $\varepsilon_v/\varepsilon_a$ is given by

$$\varepsilon_v/\varepsilon_a = [1-2\nu_{hv}+2\bar{K}(1-\nu_{hh}-n\nu_{hv})/n]/(1-2\nu_{hv}\bar{K}) \quad \text{(A4)}$$

In the case of a horizontal sample the axial and volumetric strains due to an increase in axial stress only, $\Delta\sigma'_a$, are given by

$$\varepsilon_a = \Delta\sigma'_a/nE'_v \quad \text{(A5)}$$

and $$\varepsilon_v = \Delta\sigma'_a(1-\nu_{hh}-n\nu_{hv})/nE'_v \quad \text{(A6)}$$

The strain ratio $\varepsilon_v/\varepsilon_a$ is given by

$$\varepsilon_v/\varepsilon_a = (1-\nu_{hh}-n\nu_{hv}) \quad \text{(A7)}$$

REFERENCES

Barden, L., (1963), "Stresses and Displacements in Cross-Anisotropic Soil", Geotechnique, Vol.13 No.3.

Coulthard, J.M. (1975), "Petrology of Weathered Lower Lias Clays", PhD Thesis, University of Aston in Birmingham.

Pickering, D.J. (1970), "Anisotropic Elastic Parameters for Soils", Geotechnique, Vol.20 No.3, pp271-6.

Simons, N.E., and Som, N.N., 1969, "The Influence of Lateral Stresses on the Stress Deformation Characteristics of London Clay", Proc. 7th Intern. Conf. SMFE, Mexico, Vol.1 pp369-77.

Skempton, A.W. (1954), "The Pore Pressure Coefficients A and B", Geotechnique, Vol.4 p143.

Som, N.N. (1968), "The Effect of Stress Path on the Deformation and Consolidation of London Clay", PhD Thesis University of London.

Thomas, C.P. (1973), "Mechanical Properties of Heavily Overconsolidated Clays", PhD Thesis, University of Aston in Birmingham.